ORAL/POSTER REFERENCE: ICF0705

FEM SIMULATION OF MIXED MODE CRACK PROPAGATION INDUCED BY HYDRAULIC FRACTURING

Kazushi Sato[1], Mikiyo Itaoka[2] and Toshiyuki Hashida[2]

[1] Department of Mechanical Engineering, Miyagi National College of Technology, 48 Aza–Nodayama, Shiote, Medeshima, Natori, JAPAN
[2] Fracture Research Institute, Tohoku University, 01 Aza–Aoba, Aramaki, Aobaku, Sendai, JAPAN

ABSTRACT

The hydraulic fracturing in a rock at great depth may induce a mixed mode (Mode I and II) crack propagation. In order to establish a design methodology for a geothermal energy extraction system, the prediction of the crack growth behavior is important. This paper presents a FEM model for hydraulic fracturing taking account of the mixed mode fracture.

In the FEM simulation model, the embedded crack (EC) element is employed to represent an arbitrary crack geometry due to the mixed mode crack propagation. The cohesive crack model is incorporated with a failure function for the mixed mode fracture in rock. This fracture model is implemented in the EC element. The failure function is verified by the comparison of the experimental data and numerical results.

Using the FEM model, the growth behavior of hydraulically induced crack is analyzed. The numerical results suggests that the fracture mode become the mixed mode at a great depth due to the tectonic stress. As the shear fracture mode is dominant, the crack growth tends to propagate toward the deeper direction.

KEYWORDS

Hydraulic Fracturing, Mixed Mode Fracture, Cohesive Crack Model, Embedded Crack Element

INTRODUCTION

The hydraulic fracturing is a key technology for developing a geothermal energy extraction system. In the geothermal energy system, the crack induced by the hydraulic fracturing is used for a heat exchanging surface. In order to design the geothermal energy system, a prediction of crack growth behavior induced by hydraulic fracturing is needed.

The hydraulic fracturing in a rock at great depth may induce a mixed mode (Mode I and II) crack propagation due to a tectonic stress. In order to predict the mixed mode crack propagation, the direction of the propagating crack must be analyzed. Furthermore, the crack growth is accompanied by a formation of fracture process zone.

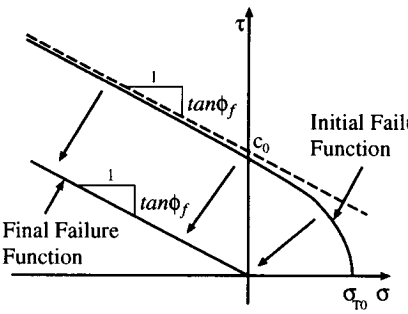

Figure 1: General shape of failure function

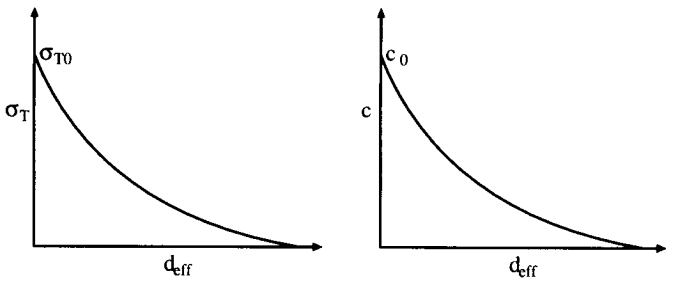

Figure 2: Softening behavior

The purpose of this study is the development of the numerical simulation code that can predict a mixed mode crack propagation with a fracture process zone during hydraulic fracturing in a deep rock mass. In order to handle both of an arbitrary crack geometry due to the mixed mode crack growth and a formation of the fracture process zone, a finite element analysis using an embedded crack (EC) element is adopted. This paper presents a FEM model for hydraulic fracturing taking account of the mixed mode fracture.

NUMERICAL MODEL

The FEM model used in this study consists of an EC element which is deal with an arbitrary crack geometry and a fracture model which represents a crack behavior of rock. This section presents a brief description of the FEM model. A detailed formulation is given in the literature [1].

The EC element has been proposed [2, 3, 4, 5] to deal with the strong displacement localization such as a crack and/or a shear bands in quasi–brittle materials. In the EC element, a crack is modeled as a displacement discontinuity within a continuum element. The major advantage of the EC element is that discrete cracks can be introduced anywhere and in any direction within the finite element mesh. According to this feature, an arbitrary crack growth can be handled without mesh refinement.

The fracture model represents the crack initiation and crack behavior in the EC element. Since the mixed mode (Mode I and II) fracture should be studied, the following failure function [6, 7] is employed as the fracture model.

$$F = \tau^2 - (c - \sigma \tan\phi_f)^2 + (c - \sigma_T \tan\phi_f)^2 \tag{1}$$

where τ and σ are the tangential and normal stress on the crack surface, respectively, c is the cohesion, ϕ_f is the angle of friction and σ_T is the tensile strength. A general shape of the failure function is shown in Figure 1. The crack initiation is determined by the initial state of the failure function. After the crack initiation, the rock exhibits a softening behavior. The softening behavior is characterized by the formation of the fracture process zone. The formation of the fracture process zone is well modeled by a cohesive crack model [8, 9]. The cohesive crack model represents the progress of fracture process by subjecting the cohesive stress to the crack surface according to the crack deformation. In this failure function, the cohesive crack model is incorporated through the parameter c and σ_T. c and σ_T are the function of a softening parameter d_{eff}, which is given by

$$d_{eff} = (d_t^2 + d_n^2)^{1/2} \tag{2}$$

where d_t and d_n are the tangential and normal relative displacement of the crack surface, respectively. The functions of c and σ_T represent softening behaviors in shear (Mode II) and tension (Mode I), as shown in Figure 2. These curves are often referred to as slip–weakening curve and tension–softening curve. As the parameters c and σ_T decrease with increasing the crack deformation, the failure function shrinks toward the final shape, which indicates a residual frictional force. During the cracking process, since the stress state on the crack surface must be maintained on the failure function, the crack follows the softening manner.

Mode II tractions generate crack slip and at the same time some induced crack opening or 'dilatancy' due to the irregularities of the crack surface. Figure 3 shows an example of the shear dilation behavior of a granite

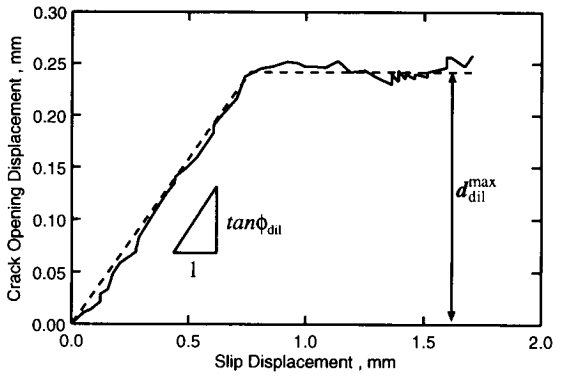

Figure 3: Shear dilation behavior

TABLE 1:
MATERIAL PROPERTIES USED

Young's modulus	41.7 GPa
Poisson's ratio	0.25
Density	2.6×10^3kg/m^3
Friction angle	40 deg
Tension–softening curve	Figure 4
Slip–weakening curve	Figure 5
Shear dilation angle	5 deg
Maximum dilatant disp.	0.60 mm

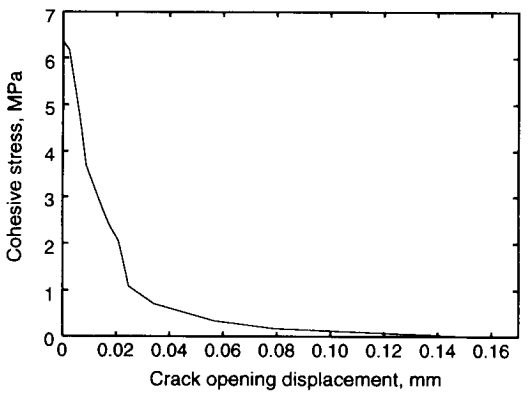

Figure 4: Tension–softening curve used

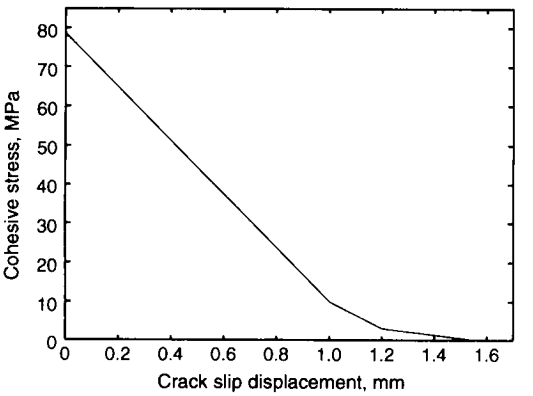

Figure 5: Slip–weakening curve used

observed in a laboratory test. It can be seen that the shear dilation indicated by the solid line in the figure is modeled as follows,

$$d_{dil} = \begin{cases} \tan\phi_{dil} \cdot d_t & (d_{dil} < d_{dil}^{max}) \\ d_{dil}^{max} & (d_{dil} \geq d_{dil}^{max}), \end{cases} \tag{3}$$

where ϕ_{dil} is the shear dilation angle and d_{dil}^{max} is the maximum dilatant displacement, as shown in the Figure 3. This shear dilation model is adopted in the fracture model in this study.

The FEM model is implemented in a 2D FEM code. A crack initiates when the stress state in an intact element reached the initial failure function. At this time, the intact element that is a generic element for an elastic analysis is replaced by the EC element with an internal crack. The crack direction can be calculated from both of the failure function and the stress state. The crack is introduced at the element centroid upon crack initiation and only one crack is allowed in each element. If the crack initiation criterion is satisfied at the centroid of a neighboring element, the crack propagates into that element. After the crack has been formed, the crack behavior is analyzed according to the fracture model.

CRACK INITIATION

Before analyzing a hydraulic fracturing, the numerical procedure used in this study should be verified. This section describes a comparison of numerical results with experimental data obtained by compression tests focusing on the crack initiation.

Numerical Procedure

A compression test under confining pressure was analyzed. Material properties used are shown in Table 1, Figure 4 and 5. These properties are measured by compression tests and direct tension tests using Iidate granite [10].

Plain strain condition was assumed. The analyzed geometry and boundary conditions are indicated in

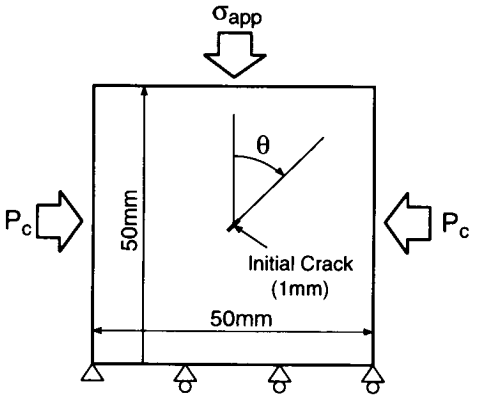

Figure 6: Boundary conditions for compression test analyses

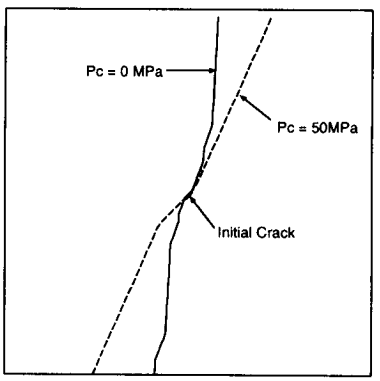

Figure 7: Final crack pattern

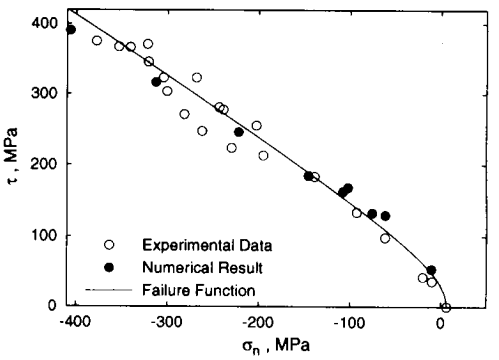

Figure 8: Crack initiation condition

Figure 6. The analyzed region was discretized using 4 node quadrilateral elements of 1mm × 1mm size. An initial crack is placed at the center of the region. The applied stress σ_{app} was raised stepwise until a crack propagate from the initial crack tip.

Numerical calculations were carried out for the condition of the confining pressure P_c varied from 0 to 200MPa and the inclination of the initial crack θ varied from 0 to 90 deg. for each confining pressure.

Failure Criterion

Crack patterns for θ = 45 deg. obtained by the numerical calculation for P_c = 0 MPa and 50 MPa are indicated in Figure 7. All the observed crack was propagated at the maximum applied stress. The crack pattern for P_c = 0 shows a growth in the direction toward the applied stress. For P_c = 50 MPa, the crack grows inclined direction, which indicates a shear fracturing. These crack growth behavior is consistent with that observed in compression tests of rocks.

A failure condition can be determined using a failure angle and a stress state when the failure was occurred. On experimental observations, the failure condition is deduced at the maximum applied stress point. Figure 8 shows a comparison of the failure condition deduced from the stress state and the crack angle observed at experiments for Iidate granite [10] and numerical results. The failure function used in the numerical calculation is also indicated for comparison. It can be seen that the failure function, which is determined by the independently measured parameters c, σ_T and ϕ_f, approximately represents the experimental data. And the numerical results follow the failure function, although small discrepancies are observed by the reason of either the softening behavior accompanied by the crack growth or the stepwise load control in the numerical procedure. These comparison results demonstrates a validity of the failure function as well as a validity of the numerical procedure. This evidence supports that the fracture behavior under high tectonic stress can be analyzed using the numerical procedure developed in this study.

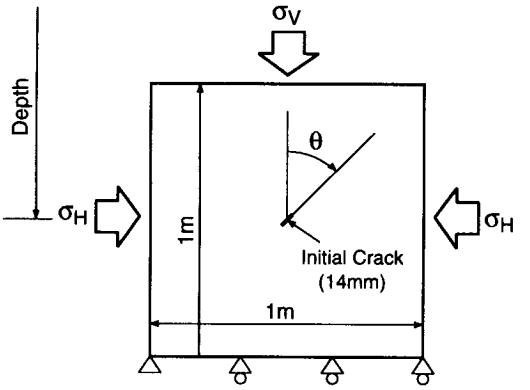

Figure 9: Boundary conditions for hydraulic fracturing analyses

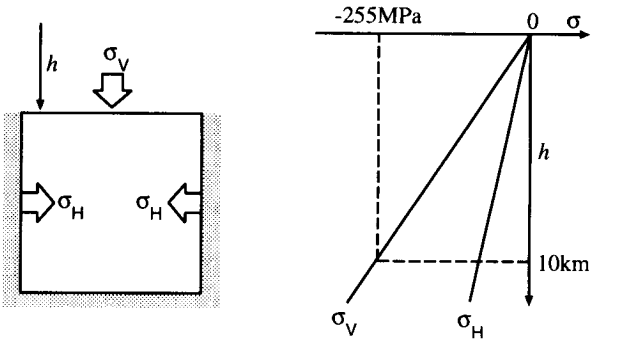

Figure 10: Tectonic stress model

HYDRAULIC FRACTURING

In order to analyze a hydraulic fracturing, a fluid flow in the rock should be calculated as well as the rock fracture. The fluid flow in the rock consists of a flow through the crack and flow into the rock mass. In this paper, the fluid flow through the crack is taken into account, although the flow into the rock mass is ignored. In this section, a growth behavior induced by hydraulic fracturing is examined focusing on the influence of tectonic stress.

Numerical Procedure

A small scall hydraulic fracturing was analyzed. Material properties are same as used in the previous section.

Plain strain condition was assumed. The analyzed geometry and boundary conditions are indicated in Figure 9. The analyzed region was discretized using 4 node quadrilateral elements of 14mm × 14mm size. An initial crack is placed at the center of the region. The inclination of the initial crack is 45 deg. The hydraulic pressure is applied into the initial crack. After the crack propagated, the fluid pressure distribution along the crack is calculated by a finite difference method.

The tectonic stress is assumed by the stress induced by the weight of rock, as follows,

$$\sigma_V = \rho g h, \tag{4}$$

$$\sigma_H = \sigma_V \cdot \nu/(1-\nu) \tag{5}$$

where ρ is the density of rock, g is the acceleration of gravity, h is the depth and ν is the Poisson's ratio. Therefore, the tectonic stress is proportional for the depth. Numerical calculations were carried out for the depth at 1, 4, 6, 8 and 10km.

Crack Growth Behavior

The crack growth pattern at 1, 6 and 10km is shown in Figure 11(a)~(c). At 1 km, the crack grows toward the vertical direction, and the upward crack is larger than the downward crack. At 10 km, the crack growth direction is inclined, and the upward crack is smaller than the downward crack. This differences of the growth behavior is the result of the change of fracture mode due to the tectonic stress.

Figure 12 indicates the stress condition at the advancing crack tip when the crack is nucleated. In the case of 1~4 km, the fracture mode is opening mode. If the opening mode dominated the fracture behavior, the crack may tend to grow upward, since the tectonic stress decreases gradually. At 6 km, the fracture mode is a mixed mode, but the opening mode seems to be dominant, according to the crack growth shown in Figure 11(b). In the case deeper than 8 km, the failure condition is on the compressive stress state. Therefore, it can be consider that the shear fracture mode dominates the crack growth behavior. As the result of this, it can be seen that the amount of the crack growth is larger in the deeper direction.

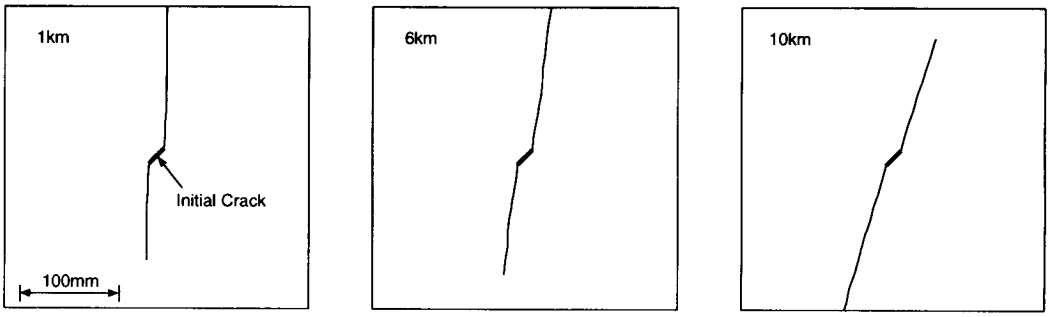

Figure 11: Crack growth pattern

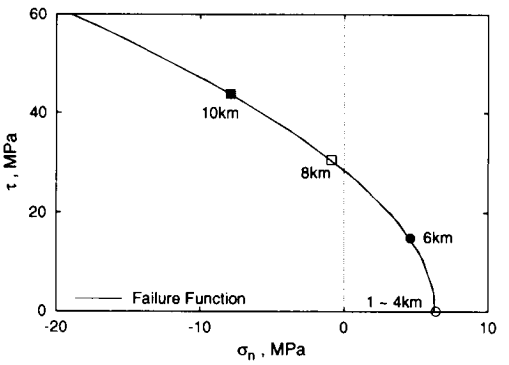

Figure 12: Stress conditions

CONCLUSION

This paper presents a brief description of a FEM model for analyzing a crack growth induced by hydraulic fracturing. In the numerical model, a mixed mode fracture is taken into account. The FEM model is verified by the comparison of the experimental data and numerical results. Using the FEM model, the growth behavior of hydraulically induced crack was analyzed. The numerical results suggests that the fracture mode become the mixed mode at a great depth due to the tectonic stress. As the shear fracture mode is dominant, the crack growth tends to propagate toward the deeper direction.

ACKNOWLEDGMENTS

The study presented in this paper was supported by The Japan Society for the Promotion of Science under "Research for Future" program (JSPS-RFTF 97P00901).

REFERENCES

1. Sato, K. and Hashida, T. (2000). *Proc. World Geothermal Congress 2000*, 3865–3870.
2. Dvorkin, E. N., Cuitino, A. M. and Gioia, G. (1990). *Int. j. Numer. Methods. Eng.*, 30, 541–564.
3. Klisinski, M., Runesson, K. and Sture S. (1991). *J. Eng. Mech.*, 117(3), 575–587.
4. Lotfi, H. R. and Shing, B. (1995). *Int. j. Numer. Methods. Eng.*, 38, 1307–1325.
5. Ohlsson, U. and Olofsson, T. (1997). *J. Eng. Mech.*, 123(10), 1027–1033.
6. Carol, I., Prat, P. C. and Lopez C. M. (1997). *J. Eng. Mech.*, 123(8), 765–773.
7. Červenka, J. (1994). PhD Thesis, Univ. of Colorado, Boulder.
8. Hillerborg, A. (1983). In: *Fractur Mechanics of Concrete*, F. H. Wittmann (Ed.)., Elsevier Science Publishers, B. V., Amsterdam, 223–250.
9. Rice, J. R. and Cleary, M. P. (1976). *Rev. Geophys. and Space Phys.*, 14, 227–241.
10. Takahashi, T. (2000). PhD Thesis, Tohoku University, Japan.